2011 IEEE/RSJ International Conference on
Intelligent Robots and Systems
September 25-30, 2011. San Francisco, CA, USA

Virtual Chassis for Snake Robots

David Rollinson and Howie Choset

***Abstract*— We present a new method of defining a body coordinate frame for locomoting snake robots. Representing the motion of snake robots from the perspective of the robot is difficult because the internal shape changes that the robot uses to locomote interact with world in a complex way. Therefore, rather than representing the system in a body frame that is static to some fixed point on a link, we instead define a body frame that is consistent with the overall shape of the robot in all configurations. We are able to define such a body frame by continuously aligning it with the principal moments of inertia taken at the center of mass of the robot. In some cases we are able to further exploit symmetry in the shape of the robot's cyclic motion (*gait*), and use non-linear optimization to more precisely align the body frame with the true axis of symmetry of the robot's shape. These shape stable body frames serve as *virtual chassis* that effectively separate the internal motion of a gait from the external motion due to that gait's interaction with the world. Furthermore, these body frames allow the motion of the robot to be described in a way that is well-aligned with one's intuitive notions of position and orientation that arise when considering the system as a whole.**

I. Introduction

Snake robots are a class of hyper-redundant mechanisms [1] consisting of kinematically constrained links chained together in series. Their many degrees of freedom allow them to navigate a wide range environments. Our group has developed modular snake robots that rely solely on their internal shape changes to locomote through their environment [2]. To simplify control of the snake's many degrees of freedom, cyclic motions, known as gaits, have been developed that undulate the snake's joints according to parameterized sine waves [3]. A survey of a wide variety of gaits and snake robot locomotion is presented in [4]. Along these lines, we have developed and implemented gaits that can traverse a variety of terrains, including flat ground and pipes, as shown in Fig. 1.

A significant challenge with snake robots involves representing motion. In particular, defining a body frame in which to intuitively model external motion in the world is difficult. Since the internal shape changes that a snake robot uses to locomote involve the entire body, no coordinate frame that is static with respect to a single point on the robot intuitively represents position and orientation of the entire robot throughout a complete gait cycle.

To illustrate this problem, consider a simple two-wheeled differential drive robot with a body frame fixed at the center of the chassis. Remotely operating such a device is an easy task because the controls, which are provided in the body coordinate frame, map intuitively into a world frame. In the case of highly articulated mechanisms like the snakes, an operator can still control the snakes with a sense of the robot's position and orientation. However, the intuition for this frame lies solely with the operator, and is drawn from observing the system as a whole rather than a single module. Similarly, we would like to formally define a body frame that is based on the configuration of the entire system rather than one that is fixed to some point. Additionally, the separation of the robot's internal shape changes from its external motions made possible by this body frame can allow much simpler motion models to accurately describe the robot's motion in the world.

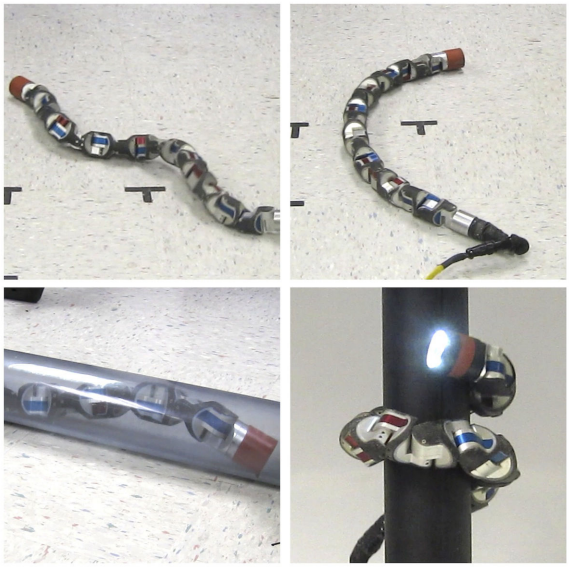

Fig. 1: Examples of snake robots executing the gaits discussed in this paper. From top left to bottom right: sidewinding, rolling, pipe crawling, and pole climbing.

This work connects the intuitive notions of overall position and orientation of the snake with the formal definitions of center of mass and principal moments of inertia of the shape of the snake. The center of mass can be calculated by averaging the x, y and z positions of the modules in an arbitrary frame, and the principal moments of inertia of the snake can be determined by taking the singular value decomposition (SVD) of the positions of all of the snake's modules. Performing these calculations for a given configuration of the snake results in a body frame that, while dynamic with respect to the pose of any individual module,

David Rollinson is a graduate student in the Robotics Institute, Carnegie Mellon University, Pittsburgh, PA, 15213 drollins@cs.cmu.edu
Howie Choset is an associate professor in the Robotics Institute, Carnegie Mellon University, Pittsburgh, PA, 15213 choset@cs.cmu.edu

is consistent with respect to the overall shape of the snake. This virtual chassis serves to separate the internal motion of a gait itself from the external motion due to that gait's interaction in the world. Furthermore, it closely matches the intuition of how one would naturally describe the overall pose of the snake.

Animations of the virtual chassis for the gaits presented in this paper are presented in the accompanying video.

II. Prior Work

There is a significant amount prior work in the study of the motion of biological snakes [5] [6] and snake robots [1] [7], these being a only selection of the works available. More recent research on both biological snakes [8] and robotic snakes [9] [10] has focused on a snake's interaction with its environment during locomotion. Our work differs significantly from these approaches in that we do not consider robot interaction with the world. Instead, our intention is to better understand and more simply represent the basic concepts of position and pose for snake robots, even before considering the effects of ground contact and friction.

Using the principal axes of a system as a way of reducing complexity has been explored in other systems. Shapere and Wilczek [11] use the center of mass and principal axes to define body frames for swimming systems. Kajita et al. [12] use the pseudo-inverse of the inertia matrix to quickly generate whole body motions where the linear and angular momenta of a humanoid robot are controlled. However, in this work the body frame for the robot is always static to some fixed point (e.g., a foot on the ground that is assumed not to move in the world frame). This convenience is not possible with snake robots as the ground contact is much more complex and it is difficult to accurately estimate what points on the snake, if any, are stationary in the world at some point in time.

In many ways, our work is inspired by the work of Hatton and Choset [13] who demonstrate that a good choice of body frame can greatly simplify motion planning. While we lack the specific constraints needed to define optimal frames in their manner, our work draws on their observation that an optimal choice of body frame is often aligned with the intuitive notions of center of mass and mean orientation.

III. Virtual Chassis

A. Gaits and Robot Kinematics

To simplify control of the 16 degrees of freedom used to locomote our robot, we rely on pre-defined undulations that are passed through the length of the snake. In our case we use parameterized sine waves that are based on Hirose's serpenoid curve [7], and its 3D extensions [14].

To provide manipulation and mobility in three dimensions, our snake robots consist of 16 modules where the joints are alternately oriented in the lateral and dorsal planes of the snake [2]. Because of this design, our framework for gaits consists of separate parameterized sine waves that propagate through the lateral (even-numbered) and dorsal (odd-numbered) joints. We refer to this framework as the *compound serpenoid curve*,

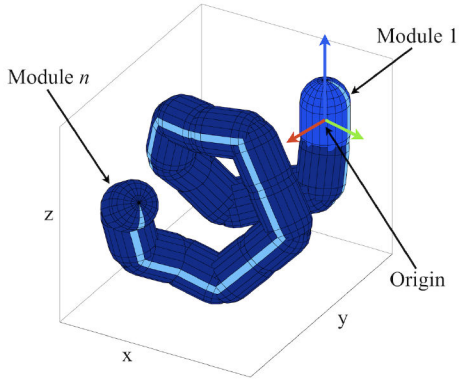

Fig. 2: Example of a starting body frame for the snake that is fixed to the head module.

$$\theta(n,t) = \begin{cases} \beta_{\text{odd}} + A_{\text{odd}}\sin(\xi_{\text{odd}}) & \text{odd} \\ \beta_{\text{even}} + A_{\text{even}}\sin(\xi_{\text{even}} + \delta) & \text{even} \end{cases} \tag{1}$$

$$\begin{aligned} \xi_{\text{odd}} &= \Omega_{\text{odd}} n + \nu_{\text{odd}} t \\ \xi_{\text{even}} &= \Omega_{\text{even}} n + \nu_{\text{even}} t. \end{aligned} \tag{2}$$

In (1) β, A and δ are respectively the angular offset, amplitude, and phase shift between the lateral and dorsal joint waves. In (2) the parameter Ω describes the spatial frequency of the macroscopic shape of the robot with respect to module number, n. The temporal component ν determines the frequency of the actuator cycles with respect to time, t.

Using the equations for the compound serpenoid curve (1) and (2), the parameters describing a given gait, and the snake's mechanical design parameters (configuration of joint axes and the distance between joints), we can generate the 3-dimensional shape of the snake from the forward kinematics of the system. Figure 2 shows an arbitrary initial frame where the origin and x, y, and z axes of the snake are defined to be the origin and respective axes of the head module.

B. Calculating the Body Frame

The overall method of deriving the virtual chassis can be thought of as performing principal component analysis (PCA) on zero-mean data. Specifically, this is done by taking the singular value decomposition (SVD) of the positions of all of the robot's modules with respect to the center of mass.

The first step to finding the virtual chassis for a given configuration is to find the geometric center of mass of the robot $\bar{x}$, $\bar{y}$ and $\bar{z}$, and construct a data matrix of the positions of the modules $\mathbf{p_i}$ measured from the center of mass (3) and (4). This matrix, $\mathbf{P}$ will be of size $n\times 3$ where each row i corresponds to the ith module in the snake,

$$\mathbf{p_i} = \begin{bmatrix} x_i - \bar{x} & y_i - \bar{y} & z_i - \bar{z} \end{bmatrix}^T \in \mathbb{R}^3 \tag{3}$$

$$\mathbf{P} = \begin{bmatrix} \mathbf{p_1}^T \\ \vdots \\ \mathbf{p_n}^T \end{bmatrix}. \tag{4}$$

After shifting the origin of the initial coordinate frame to the center of mass, the next step is to find the rotation such that the principal axes of the body frame are aligned with the principal moments of inertia of the module positions. To find this rotation we take the SVD of $\mathbf{P}$. SVD decomposes this matrix into 3 new matrices,

$$\mathbf{U}\mathbf{S}\mathbf{V}^T = \mathbf{P}. \tag{5}$$

In the decomposition, the non-zero elements of $\mathbf{S}$ are the square roots of the eigenvalues of $\mathbf{P}^T\mathbf{P}$ and describe the magnitudes of the principal moments of inertia. The columns of $\mathbf{V}$ are the eigenvectors of $\mathbf{P}^T\mathbf{P}$ and thus serve as the rotation matrix that describes the orientation of the coordinate frame aligned with the principal moments of inertia.

Problems arise when directly using $\mathbf{V}$ because the decomposition provided by SVD is only unique up to a reflection about each singular vector [15]. To ensure right-handed coordinates, at each time step $\hat{\mathbf{V}}$ is defined to be equal to $\mathbf{V}$, except that the third singular vector is defined to be the cross product of the first and second singular vectors. If desired, further sign ambiguity can be addressed at the initial time step by using some simple heuristics (e.g. making sure dot product of the first singular vector and the head module is positive).

To avoid sign flips in $\hat{\mathbf{V}}$ across later time steps, we enforce positive dot products on the first and second singular vectors at the current time step with those of the previous time step. As long as the same initial body frame was used to generate $\mathbf{P}$ and the shape changes between time steps are not drastic, the rotation described by $\hat{\mathbf{V}}$ is stable and unambiguous in sign.

Combining the rotation matrix $\hat{\mathbf{V}}$ with the center of mass $\bar{\mathbf{p}}$ we have the homogeneous transform that describes the pose of the virtual chassis in the initial coordinate frame,

$$\mathbf{T} = \begin{bmatrix} \hat{\mathbf{V}} & \bar{\mathbf{p}} \\ 0 & 1 \end{bmatrix}. \tag{6}$$

If the pose of each module is described by a homogeneous transform, left-multiplying each module's transform by $\mathbf{T}^{-1}$ converts its representation from the initial coordinate frame into the body frame of the virtual chassis.

Note that this body frame will be different with respect to the frame of the head module (and any other module in the snake) at every point in the gait cycle. What we gain in exchange for this complexity is a body frame that is instead consistent with respect to the overall shape snake across all positions of a gait cycle. In the following section we present details of the actual implementation of the virtual chassis for four different gaits that have been developed for our lab's snake robots: sidewinding, rolling, pipe crawling, and pole climbing.

IV. Implementation

A. Sidewinding

The sidewinding gait is characterized by a series of lateral and dorsal undulations that progress down the length of the snake robot as it moves [16]. The key feature in the serpenoid equations that causes this behavior is a $\pi/4$ offset in the lateral and dorsal joint angles, δ from (1). The overall shape of the snake in sidewinding can be described as a helix with an elliptical cross-section. Another way of describing the motion of sidewinding is to consider the snake to be a rolling tread on an elliptical cylinder [17]. This body shape has the property that the longest, middle, and shortest dimensions of the shape are clearly defined and are approximately orthogonal as shown in Fig. 3a.

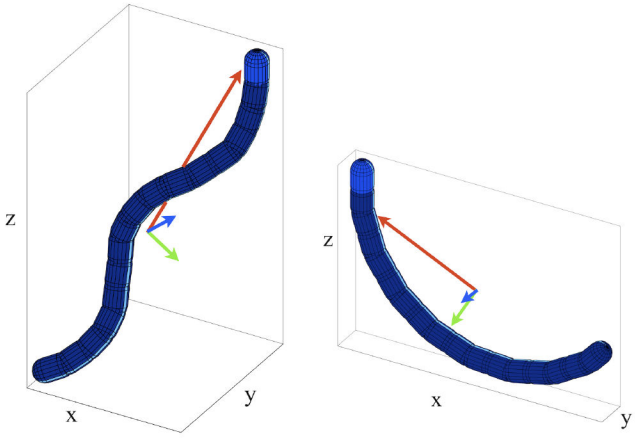

(a) Sidewinding (b) Rolling

Fig. 3: An example of the approximate axes of the virtual chassis for the sidewinding and rolling gaits.

For sidewinding, the procedure for calculating the virtual chassis follows the general procedure from Section III. At each new time step, a new $\mathbf{P}$ is calculated from the snake robot's joint angles and a new body frame is defined. The transformation of sidewinding from an initial fixed frame to the virtual chassis body frame is shown in the appendix.

B. Rolling

In the basic rolling gait the modules form an arc of constant curvature that is swept through the lateral and dorsal joints. The key to this constant curvature is that the spatial frequency Ω in (2) is set to 0, and the offset between the lateral and dorsal joint angles, δ from (1), is set to $\pi/2$ radians.

As the snake cycles through the gait on flat ground, the arc remains level on the ground and the snake rolls either toward or away from the center of the arc, depending upon which direction the waves are traveling through the joints. Like sidewinding, the shape of the snake in rolling has clearly defined longest, middle, shortest dimensions to its shape that again are approximately orthogonal (Fig. 3b).

For this gait we align the first, second, and third principal moments of inertia respectively with the x, y, and z axes of the body frame. The procedure for calculating the virtual chassis for rolling follows the general procedure. The transformation of rolling from an initial fixed frame to the virtual chassis body frame is shown in the appendix.

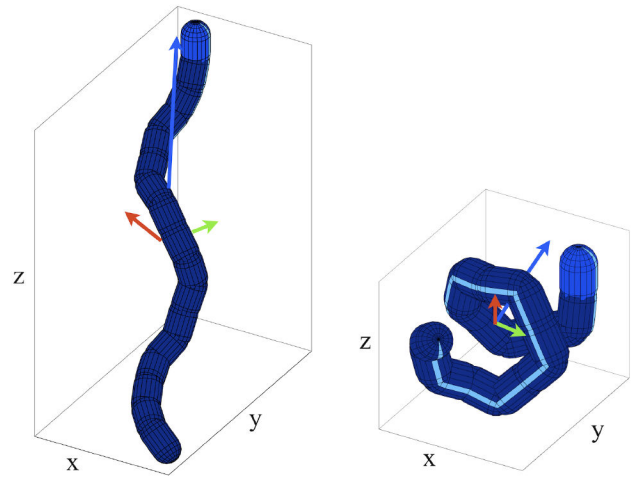

(a) Helix - Pipe Crawling (b) Helix - Pole Climbing

Fig. 4: An example of the approximate axes of the virtual chassis for a position in the pipe crawling and pole climbing gaits.

C. Helix - Pipe Crawling

The helix gait is in the family of rolling gaits. Like the simple rolling gait, it is characterized by a $\pi/2$ offset in the lateral and dorsal joint angles δ. However, in this case a non-zero spatial frequency Ω causes the base shape of the gait to form a cylindrical helix, rather than an arc. Pipe crawling is a parametrization of helix in which Ω creates approximately 1.5 wave cycles over the length of the snake.

The shape of the snake in pipe crawling has a clearly defined longest direction, corresponding to the first principal moment of inertia, as seen in Fig. 4a. However, in this gait the second and third moments of inertia are somewhat ambiguous. This result makes intuitive sense, since for a true cylinder the second and third movements are exactly equal. In our case, the finite number of modules in the snake inherently weights one side of the helix more than the other, and the general procedure will still find a stable solution for all three moments of inertia.

The resulting body frame using the general procedure is stable with respect to the shape of the snake robot. However, since this gait is used specifically for locomoting on the inside of pipes (bottom left of Fig. 1) we can make further refinements. Specifically, we can exploit the known constraints of the environment and define a more useful body frame that is better aligned with the true centerline of the helix.

To find the true centerline of the snake, we take the initial solution from SVD and use it as the starting point of optimization using the Nelder-Mead simplex search [18]. Intuitively, we would like to minimize the difference of the distances of all the modules in snake to some centerline. The distance d_i of a point $\mathbf{p_i}$ to a line defined by $\mathbf{a}+\mathbf{v}s$ is defined as:

$$d_i = |(\mathbf{a} + ((\mathbf{p_i} - \mathbf{a}) \cdot \mathbf{v})\mathbf{v} - \mathbf{p_i})| \tag{7}$$

The objective function for optimizing the centerline parameters $\mathbf{a}$ and $\mathbf{v}$ is the sum-squared error of the distance from each module to the centerline d_i compared to the mean distance of all the modules to the centerline $\bar{d}$.

$$\text{error} = \sum_{i=1}^{n} (d_i - \bar{d})^2 \tag{8}$$

Because this objective function is non-convex, random restarts in the vicinity of the initial SVD solution are used to ensure that the optimization does not converge in a local minimum that does not reflect the true centerline of the snake robot's shape.

For this gait, the z axis is chosen to align with the optimized centerline vector $\mathbf{v}$. An arbitrary reference module (in our case, the middle module) is chosen to define the frame's rotation about the centerline. This is achieved by aligning the y axis with the vector that describes the line perpendicular from the chosen reference module to the centerline. Lastly, the desired x axis is calculated from the cross product of the z and y axes, to ensure a right-handed coordinate frame. The final transformation of pipe crawling from an initial fixed frame to the virtual chassis body frame after optimization is shown in the appendix.

D. Helix - Pole Climbing

Pole climbing is a different range of parametrizations of the helix gait in which the diameter of the helix is much wider and the pitch is less steep. This is caused by the gait's comparatively larger values for amplitude A, and smaller values of spatial frequency Ω.

As in pipe crawling, the coordinate frame can again be optimized beyond what is provided by SVD. In fact, it becomes even more beneficial as the misalignment of the first principal moment of inertia with the true centerline of the snake's helix is much more pronounced. This is effect primarily attributable to the 'longest' direction of the snake's shape becoming more ambiguous, as the larger diameter of the helix starts to approach the overall length of the helix (Fig. 4b). The virtual chassis body frame for pole climbing is calculated in the same secondary optimization step as pipe crawling, and the result is shown in the appendix.

The pole climbing gait is the clearest example of the intuition that can be gained by representing motion using the virtual chassis. While executing an entire cycle of the gait, the overall position of the modules remain stationary in the body frame and the body frame exploits the symmetry of the snake's shape and the environment. If we now wish to represent the motion of the snake robot as it translates along or rotates about a pole in some world frame, these motions can now be closely approximated by simple translations along and rotations about only the z axis of the body frame.

V. Conclusions

The virtual chassis is a framework that allows one to represent a snake robot's world motion in a simplified and intuitive manner. By exploiting the property that the overall shapes of gaits are relatively stable throughout an entire gait cycle, we have introduced a way of representing the motion of the

snake in a way that inherently separates internal motion due to the shape changes of a gait from external motion caused by a gaits interaction with the world. Through this separation of motions, these body frames mirror the natural notions of position and pose of the snake robot that previously rested only with a human operator. A general method that uses SVD to determine the virtual chassis body frame for any shape is presented. For case of the helix gait, the body frame is further refined by using non-linear optimization to better align the body frame with true centerline of the snake robot's shape.

VI. Future Work

1) Gait Transitions: Since the general method for determining the virtual chassis body frame can be applied to any shape configuration of the snake robot, it could potentially be used to better understand gait transitions. Because gait transitions depart from the intuitive structure provided by regular gait motions, they can be a challenge for both control and estimation. It is likely that the virtual chassis could help better define and estimate the pose of the snake throughout a transition.

2) Real-time Implementation: In the cases where the virtual chassis can be found from SVD alone, finding the frame given the snake's joint angles can be calculated fast enough to use in real time (our latest snakes report feedback at approximately 35 Hz). However, in the case of both pipe crawling and pole climbing, the non-linear optimization step slows the body frame calculations considerably. For this reason we are pursuing the idea of calculating lookup tables for the body frames sorted by gait parameters. In the case of these gaits the the table would require three lookup parameters from the gait equations (1) and (2): temporal position in the gait cycle ωt, amplitude A, and spatial frequency Ω. To make use of such a table, the challenge now becomes accurately fitting gait parameters to the measured joint angles provided in the feedback from the snake.

3) Fitting Gait Parameters to Feedback: When operating the snake robots in the real world, the servos actuating the joints often do not match their commanded positions. Comparing the actual angles of each joint and to their commanded angles provides feedback that can be used in controlling the snake. However, just as we use parameterized gaits to reduce complexity and provide intuitive control of the system, we would also like use them to more intuitively represent feedback. The problem of determining the gait parameters that best describe the actual shape of the snake is one that lies in the realm of state estimation. There are many methods that can be used to fit gait parameters to feedback data in real time, including various types of Kalman filters. We are currently exploring the use of an extended Kalman filter (EKF) to perform state estimation based on feedback from the snake robot, where the state consists of only the gait parameters and the joint angles are treated as measurements that update the state estimate.

VII. Acknowledgements

The authors would like to acknowledge the help provided by the members of the Biorobotics Lab and the Robotics Institute, in particular, Ross Hatton, Matt Tesch, Austin Buchan, Mike Schwerin and Ben Brown.

Appendix: Gait Montages

The appendix contains montages of the body frames for each of the gaits described in Section IV. Each gait is shown in five different positions spaced evenly throughout one complete gait cycle. The top row of images for each gait shows the pose of the snake in a frame where a single module is fixed as the origin. The bottom row for each gait shows the pose corresponding to the virtual chassis at that same point in the gait cycle.

References

[1] G. Chirikjian and J. Burdick, "Kinematics of hyper-redundant locomotion with applications to grasping," *International Conference on Robotics and Automation*, 1991.

[2] C. Wright, A. Johnson, A. Peck, Z. McCord, A. Naaktgeboren, P. Gianfortoni, M. Gonzalez-Rivero, R. Hatton, and H. Choset, "Design of a modular snake robot," *Proceedings of the IEEE International Conference on Intelligent Robots and Systems*, October 2007.

[3] M. Tesch, K. Lipkin, I. Brown, A. Peck, J. Rembisz, and H. Choset, "Parameterized and scripted gaits for modular snake robots," *Advanced Robotics*, 2009.

[4] A. A. Transeth, K. Y. Pettersen, and P. l. Liljebäck, "A survey on snake robot modeling and locomotion," *Robotica*, vol. 27, p. 999, Mar. 2009.

[5] J. Gray, "The mechanism of locomotion in snakes," *Journal of Experimental Biology*, vol. 23, pp. 101–123, December 1946.

[6] B. C. Jayne, "Kinematics of terrestrial snake locomotion," *Copiea*, no. 4, pp. 915–927, 1986.

[7] S. Hirose, *Biologically Inspired Robots*. Oxford University Press, 1993.

[8] D. Goldman and D. Hu, "Wiggling through the world," *American Scientist*, vol. 98, pp. 314–393, July 2010.

[9] A. A. Transeth, R. I. Leine, C. Glocker, and K. Y. Pettersen, "3-d snake robot motion: Nonsmooth modeling, simulation, and experiments," *IEEE Transactions on Robotics*, vol. 24, pp. 361–376, April 2008.

[10] A. A. Transeth, R. I. Leine, C. Glocker, and K. Y. Pettersen, "Snake robot obstacle-aided locomotion: Modeling, simulations and experiments," *IEEE Transactions on Robotics*, vol. 24, pp. 88–104, February 2008.

[11] A. Shapere and F. Wilczek, "Geometry of self-propulsion at low reynolds number," *Geometric Phases in Physics*, January 1989.

[12] S. Kajita, F. Kanehiro, K. Kaneko, K. Fujiwara, K. Harada, K. Yokoi, and H. Hirukawa, "Resolved momentum control: Humanoid motion planning based on the linear and angular momentum," *Intelligent Robots and Systems*, October 2003.

[13] R. L. Hatton and H. Choset, "Geometric motion planning: The local connection, Stokes's theorem, and the importance of coordinate choice," *The International Journal of Robotics Research*, 2011.

[14] H. Ohno and S. Hirose, "Design of slim slime robot and its gait of locomotion," *Proceedings 2001 IEEE/RSJ International Conference on Intelligent Robots and Systems.*, pp. 707–715, 2001.

[15] R. Bro, E. Acar, and T. Kolda, "Resolving the sign ambiguity in the singular value decomposition," *Journal of Chemometrics*, vol. 22, no. 2, pp. 135–140, 2008.

[16] J. Burdick, J. Radford, and G. Chirikjian, "A sidewinding locomotion gait for hyper-redundant robots," *Robotics and Automation*, vol. 3, pp. 101–106, 1993.

[17] W. Mosauer, "A note on the sidewinding locomotion of snakes," *The American Naturalist*, vol. 64, pp. 179–183, March 1930.

[18] A. Nelder and R. Mead, "A simplex method for function minimization," *Computer Journal*, vol. 7, pp. 308–313, 1965.

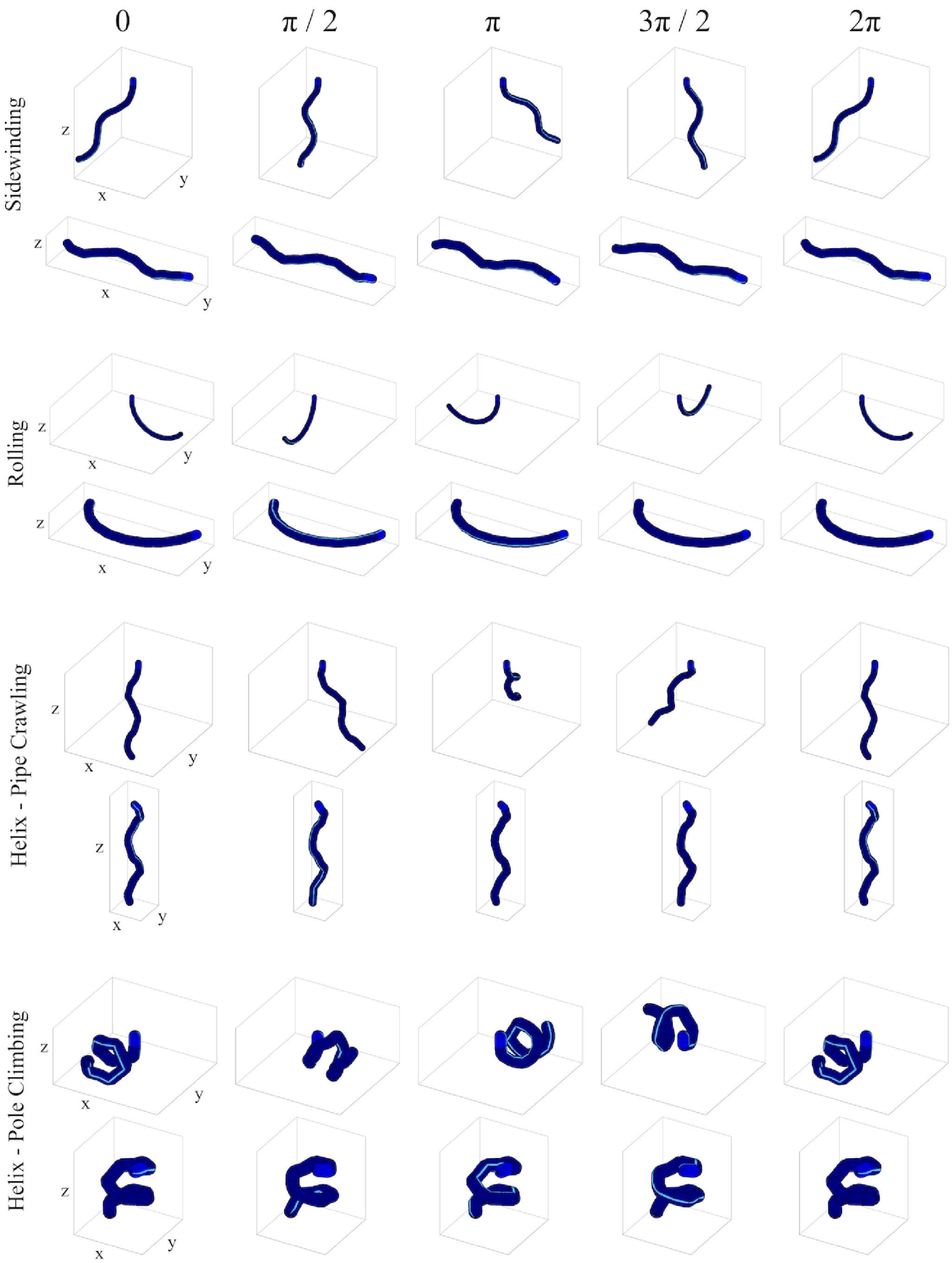
0
π / 2
π
3π / 2
2π
Sidewinding
Rolling
Helix - Pipe Crawling
Helix - Pole Climbing
z
x
y